Clays and Clay Minerals, Vol. 61, No. 1, 26–33, 2013.

STRUCTURE AND PHOTOLUMINESCENCE OF COMPOSITES BASED ON CdS ENCLOSED IN MAGADIITE

YUFENG CHEN*, GENSHENG YU, FEI LI, AND JUNCHAO WEI

Department of Chemistry, Nanchang University, Jiangxi 330031, P.R. China

Abstract—In order to extend the application of magadiite to optical fields (rather than the usual focus on adsorption, catalysis, ion exchange, *etc.*), a magadiite-CdS (Mag-CdS) composite was synthesized from Na-magadiite by ion exchange. Various techniques were used to characterize the composite. X-ray diffraction results indicated that the Mag-CdS composite retained the host magadiite structure in spite of decrease in the intensity of the X-ray diffraction peak of the host magadiite. The analytical results confirmed the formation of the Mag-CdS composite, along with the modification of the optical properties of CdS by the host magadiite.

Key Words—CdS Nanoparticles, Composites, Magadiite, Photoluminescence.

INTRODUCTION

Magadiite ($Na_2Si_{14}O_{29}{\cdot}xH_2O$) belongs to the family of layered Na silicates which includes makatite, kanemite, kenyaite, and octosilicate. It was first described by Eugster (1967) who found it, together with kenyaite, in lake beds at Lake Magadi, Kenya. Recent studies of magadiite have focused mainly on adsorption (Guerra *et al*., 2010), cation exchange (Bi *et al*., 2012), intercalation (Zhen and Pinnavaia, 2003), and modification and organization of guest species (Supronowicz *et al.*, 2012; Macedo *et al.*, 2007; Díaz *et al.*, 2007), *etc*. The modification or organization of guest molecules into Na-magadiite layered hosts offers a variety of applications, such as adsorbents (Nunes *et al.*, 2011), catalysts (Park *et al.*, 2009), cation exchangers, molecular sieves (Sun *et al.*, 2009), luminescent materials (Mizukami *et al.*, 2002; Ogawa *et al.*, 2010), optical recording materials (Ogawa and Kuroda, 1995), and separation media (Centi and Perathoner, 2008).

Nanoparticle CdS is a representative of the II−VI group semiconductors with extensive applications in electro-luminescence devices, photocatalysis, and biological sensors (Sun *et al.*, 2008; Rayevska *et al.*, 2010; Xu *et al*., 2012; Freeman *et al*., 2007). Because of the aggregation of CdS nanoparticles and the potential for oxidation, attempts have been made to improve the stability of the CdS nanoparticles by incorporating them into organic polymers (Li *et al*., 2005) or inorganic materials (Rosa-Fox *et al*., 2003; Kryukov *et al*., 1998; Chang *et al*., 1994). Though much attention has been focused on CdS nanoparticles capped by organic molecules or enclosed in a polymer matrix, which not only maintains the optical properties of the CdS but effectively protects the CdS from environmental perturbation (Rosa-Fox *et al*., 2003; Kryukov *et al*., 1998), CdS nanoparticles embedded in inorganic host materials are still worthy of study because of the greater stability of the inorganic compared with the organic materials in some special applications. Several studies of the optical properties of CdS revealed that major luminescence effects were associated with the incorporation in host materials (Shen *et al*., 2008; Jyothy *et al*., 2009). For this reason, magadiite, which has a layered structure, is thermally stable, and is resistant to common acids, bases, and oxidants, was selected here to enclose the CdS nanoparticles to form a CdS/magadiite composite. A ZnO-magadiite composite was synthesized (Ozawa *et al*., 2009) using magadiite and $Zn(NO_3)_2$ as reactants, and the size of ZnO particles as a function of heat-treatment temperatures was investigated. Here, a composite based on CdS nanoparticles enclosed in magadiite was prepared using magadiite and $Cd(NH_3)_4^{2+}$ as reactants in a basic medium that facilitated ion exchange. The optical properties of the composite were investigated. The results indicated that the optical properties of CdS nanoparticles incorporated in magadiite were quite different from those of pure CdS particles. The Mag-CdS composite should be more resistant to acids than pure CdS particles and more thermally stable than CdS composites enclosed in organic polymers. The Mag-CdS composite is, therefore, a possible candidate for use as an electro-luminescent material.

EXPERIMENTAL

Na-magadiite was synthesized by reaction of the SiO_2–NaOH–Na_2CO_3 system under hydrothermal conditions (Kwon *et al.*, 2005). At 150ºC, the reaction was carried out in a sealed, Teflon-lined autoclave with a silica gel solution (14 mL of H_2SiO_3 and 127 mL of H_2O), NaOH

* E-mail address of corresponding author:
yfchen@ncu.edu.cn
DOI: 10.1346/CCMN.2013.0610103

(0.510 g), and Na_2CO_3 (2.690 g) as the reactants. After reaction for 96 h, the product was filtered, washed with deionized water, and dried at 40ºC for 12 h. The Na-magadiite sample obtained was labeled 'Mag'. To introduce CdS nanoparticles into the interlayer space of Mag, a two-step process was used. At first, the ion-exchange method was adopted, *i.e.* Mag (1.027 g) was added to $Cd(NH_3)_4^{2+}$ aqueous solution (0.2 M, 100.0 mL) which was prepared by reaction of $CdCl_2{\cdot}5/2H_2O$ with concentrated NH_3 solution, and stirred for 3 days at room temperature. The pH of the mixed suspension was 12.0; hydrolysis of $Cd(NH_3)_4^{2+}$ could be avoided at this pH (Bases and Mesmer, 1976). A portion of the sediment from the mixed suspension was then filtered, washed, and dried at 40ºC for 12 h. The dried product was labeled as Mag-Cd. The remainder of the sediment was filtered, washed, and dispersed quickly (~2−3 min) into deionized water (100 mL) to form a new suspension in order to remove excess $Cd(NH_3)_4^{2+}$ (which can react with Na_2S to form CdS outside the magadiite) (Vorokh *et al.*, 2008). Finally, Na_2S (0.1 M, 20 mL) solution was added gradually to the new suspension and stirred continuously. The Mag-CdS composite was obtained after the precipitate was filtered, washed, and dried at 40ºC for 12 h.

The pure CdS particles were prepared by the same method as mentioned above, *i.e.* Na_2S solution (0.1 M, 20 mL) was added to $Cd(NH_3)_4^{2+}$ solution (0.2 M, 25 mL), and stirred continuously. The CdS precipitate was filtered, washed, and dried at 40ºC for 12 h.

An environmental scanning electron microscope equipped with energy dispersive X-ray analysis (SEM-EDX XL30 ESEM FEG, Philips, Genesis 2000, The Netherlands) was used for morphological analysis of the surface structure and the compositional analysis of the samples for Na, Cd, Si, O, and S, with an accelerating voltage of 20 kV for EDX microanalysis. H elemental analysis was performed using a CHN Element Analyzer (Elementar Vario EL, Hanau, Germany). Powder X-ray diffraction (XRD) patterns were measured on a Bruker D8 Focus diffractometer using CuKα radiation (Bruker, Karlsruhe Germany). All the samples were scanned in the range 2−70º2θ at a scan rate 2º2θ/min. Fourier-transform infrared (FTIR) spectra were recorded using a Shimadzu IR Prestige-21 FTIR spectrometer (Shimadzu Company, Chiyoda-ku, Tokyo, Japan). Samples were prepared using the standard KBr disc method.

Thermogravimetric (TG) and differential thermal analysis (DTA) data were collected using a synchronous thermal analyzer (STA-200, Dazhan, Jiangsu, China), in a dynamic atmosphere using dry N_2 purge gas, with heating from room temperature up to 800ºC at a rate of 10ºC/min. The optical properties were characterized using photo-luminescent spectra (FL, F-7000, Hitachi Limited Corporation, Chiyoda, Tokyo Japan) and UV-vis trans-mission spectroscopy (U-4100 Spectrophoto-meter, Hitachi Limited Corporation, Chiyoda, Tokyo, Japan). Transmission electron microscopy (TEM) (JEM-2010, JEOL Company, Akishima, Tokyo, Japan) was used to examine the morphologies and estimate the sizes of the CdS nanoparticles enclosed in the magadiite.

RESULTS AND DISCUSSION

The chemical composition of the Na-magadiite prepared here was obtained by combining the results of CHN elemental analysis, SEM-EDX compositional analyses (Figures 1 and 2), and TG analyses (Figure 3). The SEM-EDX compositional analyses of Mag and Mag-CdS (Figure 1, Table 1) revealed the molar ratio of Na:Si:O to be 1.0:7.0:18.1 for the Mag, and the morphological changes of the samples on the basis of SEM images (Figure 2). According to the thermogravimetric curve, Na-magadiite lost 9.2% of its total weight as water below 145ºC, which was mainly due to interlayer water (Aline and Alexandre, 2009). In light of the EDX analysis, CHN element analysis, and weight loss, as well as the charge-balance principle, an empirical composition for the Na-magadiite prepared was estimated to be $Na_{1.0}Si_{7.0}O_{13.0}(OH)_3{\cdot}xH_2O$ (x = 2.14), which compared favorably with the approximate composition of $NaSi_7O_{13}(OH)_3{\cdot}3H_2O$ suggested by previous workers (Eugster, 1967; Schwieger and Lagaly, 2004; McAtee *et al.*, 1968). By the same method, the molar ratio of Na:Cd:Si:S:O presented in the Mag-CdS composite was estimated to be

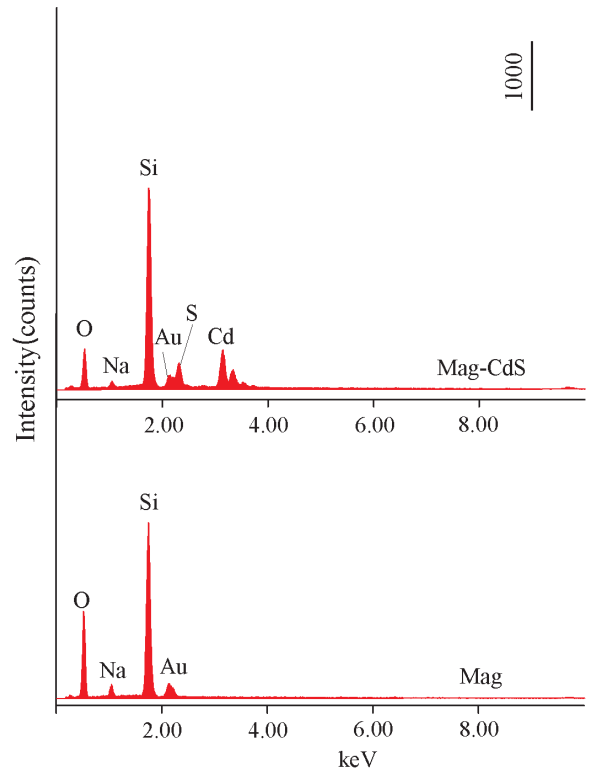

Figure 1. SEM-EDX results of Mag and Mag-CdS.

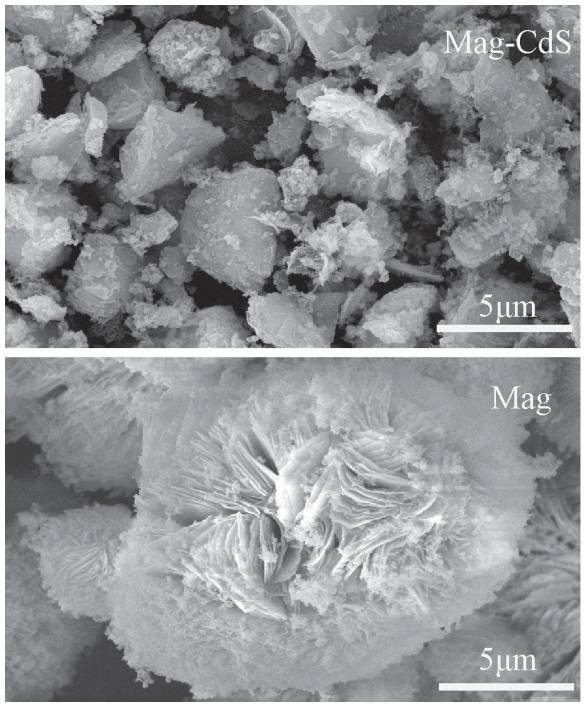

Figure 2. SEM images of Mag and Mag-CdS.

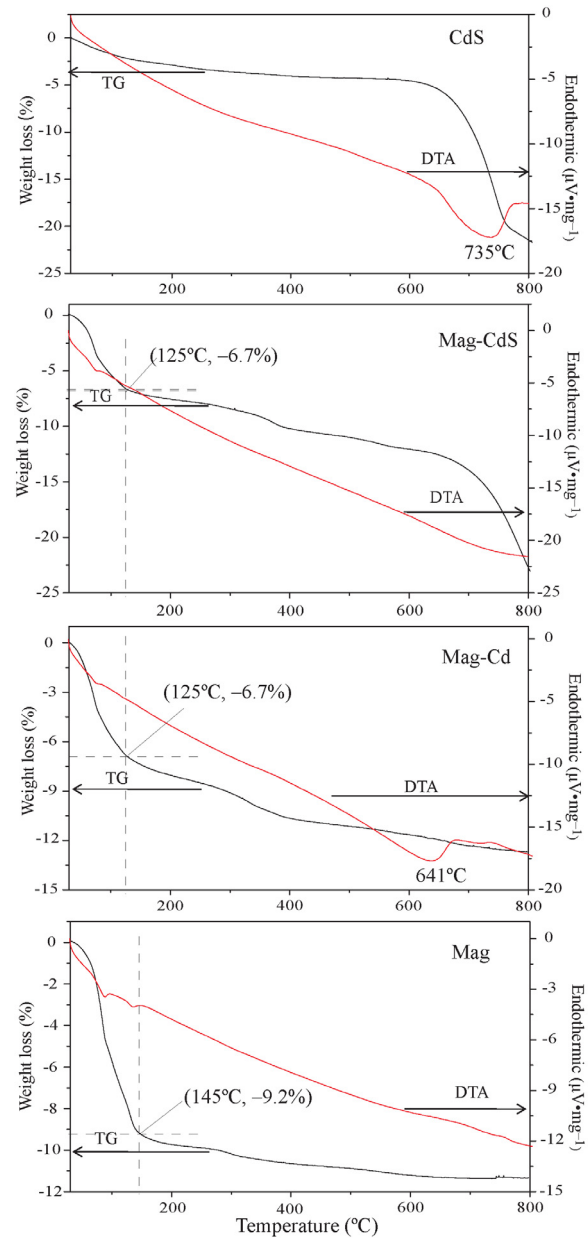

Figure 3. TG-DTA curves of Mag, Mag-Cd, Mag-CdS, and CdS.

0.28:0.82:7.0:0.46:17.87. The molar ratio of Cd:S (0.82:0.46) in the composite was not close to the expected value of 1:1, indicating excess Cd(II). The excess Cd(II) would compensate for layer charge. Allowing for the charge balance between the layers and interlayer guests, the empirical composition of the composite was estimated to be $Na_{0.28}Cd_{0.36}Si_{7.0}O_{13.0}(OH)_3\cdot(CdS)_{0.46}\cdot xH_2O$ (x = 1.87). The Au signal detected was attributed to Au electroplate.

X-ray diffraction patterns of Mag showed a d_{001} reflection corresponding to a basal spacing of 15.6 Å (Figure 4). This interlayer spacing was in agreement with values in the literature (Schwieger and Lagaly, 2004). Based on the XRD data for the Mag sample and taking into account information provided by Schwieger and Lagaly (2004), all the reflections could be indexed as shown in Figure 4. The cell parameters of Mag were refined as a = 7.272(3) Å, b = 7.297(2) Å, c = 15.684(6) Å, and β = 96.6(5)º, which values were similar to those (a = 7.25 Å, b = 7.25 Å, c = 15.69 Å, β = 96.8º) given by Schwieger and Lagaly (2004). After intercalation of $Cd(NH_3)_4^{2+}$ ions into magadiite, the reflections of the Mag-Cd (Figure 4) were less intense than those of the pure ions. However, as far as the positions of peaks were concerned, the intercalated samples still had peaks corresponding to Na-magadiite, indicating that the structure was unaffected by the introduction of $Cd(NH_3)_4]^{2+}$ ions. Moreover, the intercalation of $Cd(NH_3)_4^{2+}$ ions into magdiite resulted in no significant change in the basal spacing. In an earlier study on the intercalation of $[Pt(NH_3)_4]^{2+}$ and $Co(sep)^{3+}$ ions into Na-magadiite, no change was reported in the basal spacing either (Schwieger *et al*., 2004; Daily and Pinnavaia, 1992). Moreover, when the loading of $[Pt(NH_3)_4]^{2+}$ or $Co(sep)^{3+}$ ions increased, the intensity of the 001 (5.6º2θ) peak decreased. Similarly, a remarkable difference in the intensity of the peak at 5.6º2θ was noted, the intensity of which decreased with intercalation of $Cd(NH_3)_4^{2+}$ into magadiite, while the peak position remained unchanged. The decrease in the intensity of the peak at 5.6º2θ suggested that $Cd(NH_3)_4^{2+}$ ions were intercalated within the interlayer spaces. After introduction of S^{2-} to Mag-

Table 1. Chemical composition of Mag and Mag-CdS.

Samples	Elements	Wt.%	Molar ratio (%)	Molar ratio/formula/weight loss
Mag	OK	69.35	54.28	Na:Si:O:H=1.0:7.0:18.1:7.3 $Na_{1.0}Si_{7.0}O_{13.0}(OH)_3{\cdot}xH_2O$ (x = 2.14) H_2O loss = 9.2% (~25−145ºC)
	NaK	5.49	2.99	
	SiK	23.42	20.94	
	H	1.74	21.78	
Mag-CdS	OK	56.77	53.87	Na:Cd:Si:S:O:H = 0.28:0.82:7.0:0.46:17.87:6.74 $Na_{0.28}Cd_{0.36}Si_{7.0}O_{13.0}(OH)_3{\cdot}(CdS)_{0.46}{\cdot}xH_2O$ (x = 1.87) H_2O loss = 6.7% (~25−125ºC)
	NaK	1.28	0.84	
	SiK	19.46	21.10	
	SK	2.92	1.39	
	CdL	18.23	2.48	
	H	1.34	20.32	

Na, Cd, Si, S, and O analyzed by EDX; H obtained from CHN element analysis and TG.

Cd, the final product, Mag-CdS, also retained the layered structure of the host magadiite. Therefore, both the Mag-Cd and Mag-CdS had similar interlamellar basal spacings to those of the initial magadiite (15.6 Å), which may be attributed to two opposing effects: the increasing interlayer spacing caused by the introduction of $Cd(NH_3)_4^{2+}$ or CdS into the Mag and the decreasing interlayer spacing brought about by the loss of interlayer water. These two opposing effects occurred simultaneously, leading to invariable spacing. In addition, the XRD pattern of the pure CdS showed no obvious peaks, suggesting that it was amorphous. Reflections attributed to CdS were not observed in the XRD patterns of Mag-CdS. Therefore, the CdS enclosed in the magadiite may have been amorphous.

The thermal analyses of Mag, Mag-Cd, Mag-CdS, and CdS (Figure 3) suggested that the TG-DTA curves of Mag-Cd and Mag-CdS were very different from those of Mag and CdS. This expected difference may be associated with the use of the $Cd(NH_3)_4^{2+}$ cations or CdS nanoparticles were possibly inserted into the lamellar space. As shown in TG curves, Mag exhibited a rapid mass loss of 9.2% up to 145ºC because of loss of interlayer water (Aline and Alexandre, 2009). After ion exchange with $Cd(NH_3)_4^{2+}$ at room temperature, the Mag may have lost some interlayer water molecules owing to intercalation of $Cd(NH_3)_4^{2+}$. So the mass loss up to 145ºC for Mag-Cd was ~6.7%. Although the TG-DTA curves changed after the introduction of CdS nanoparticles to the Mag, the mass loss of 6.7% up to 145ºC for the Mag-CdS composite persisted. Moreover, the TG-DTA curves of Mag-CdS composite were the same as those of Mag and CdS. These results confirmed the formation of the Mag-CdS composite.

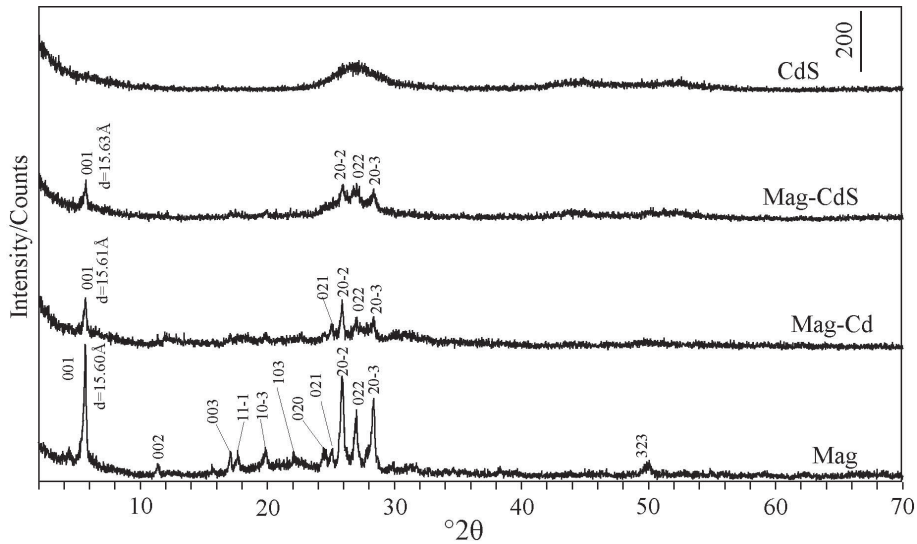

Figure 4. XRD patterns of Mag, Mag-Cd, Mag-CdS, and CdS.

Infrared spectra of Mag, Mag-Cd, Mag-CdS, and CdS (Figure 5) showed that, for Mag-Cd and Mag-CdS, all of the IR bands observed appeared at different frequencies from those in the Mag and CdS, with the exception of the bands at 3445 and 1635 cm^{-1} which were attributed to the presence of the O–H stretching and bending modes of silanol groups and water molecules (distinguishing between them is difficult) (Motke *et al.*, 2002). For the Mag, the antisymmetric stretching modes of Si–O–Si bridges were observed at 1107 cm^{-1} (Nunes *et al.*, 2011), while the band at 458 cm^{-1} was associated with the very strong symmetric stretching vibrations of Si–O–Si bridges (Huang *et al.*, 1999). The vibrational mode near 782 cm^{-1} was attributed to the mordenite bending mode of Si–O–Si mixed with Si–Si motion (Huang *et al.*, 1999; Laughlin and Joannopoulos, 1977). With respect to the IR spectra of the intermediate product, Mag-Cd, and the final product, Mag-CdS, distinct changes in the region 458–1107 cm^{-1} were found. The band at 1107 cm^{-1} shifted to 1083 cm^{-1} and this was assigned to the stretching modes of terminal Si–O^{-} bonds from *Q*3 units (Huang *et al.*, 1999). The bands between 663 and 446 cm^{-1} were associated with the symmetric stretching vibrations of Si–O–Si bridges (Huang *et al.*, 1999). All these results suggested that the composite formed was based on the incorporation of CdS in the magadiite.

Photoluminescence (PL) measurements (Figure 6) were taken at room temperature. The PL excitation spectrum of the pure CdS detected at 556 nm (Figure 6I) showed a broad excitation band ranging from 445 to 340 nm. The emission spectra of the pure CdS were obtained under excitations at 320, 340, 350, 365, 370, and 445 nm (Figure 6II). A weak, high-energy peak at 470 nm and a broad peak centered at ~556 nm were observed in all the emission spectra of the CdS. The sources of the bands are the subject of some debate. Most researchers believe that the high-energy peak at 470 nm is due to near-band-edge emission while the strong, broad, and asymmetrical peak centered at ~556 nm is usually attributed to recombination of trapped charge carriers at surface defects due to either sulfur vacancies or cadmium vacancies (Zhao *et al.*, 2012; Rai and Bokatial, 2011). Some researchers consider, however, that the peak at ~556 nm corresponds to the band gap of CdS and the weak emission peak at 470 nm is attributed to a higher-level transition in CdS crystallites (Wang *et al.*, 2002; Wei *et al.*, 2005).

The emission spectra of the Mag-CdS composite (Figure 7) revealed a strong, broad peak centered at

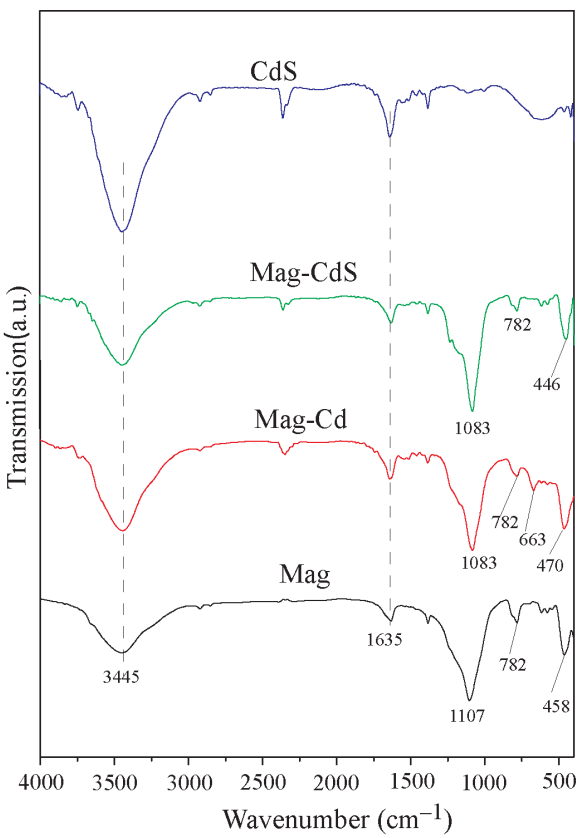

Figure 5. FTIR spectra of Mag, Mag-Cd, Mag-CdS, and CdS.

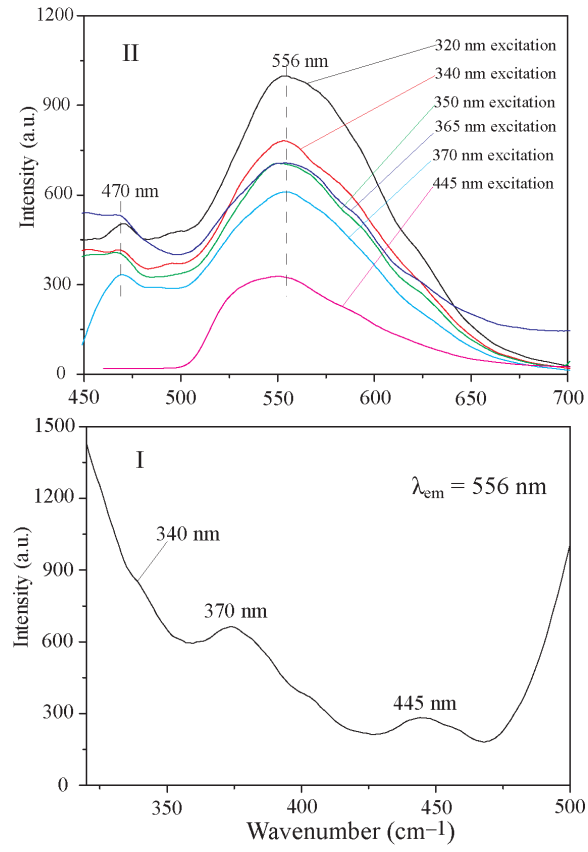

Figure 6. Excitation spectrum of CdS (λ_{em} = 556 nm) and emission spectra of CdS under different excitation wavelengths.

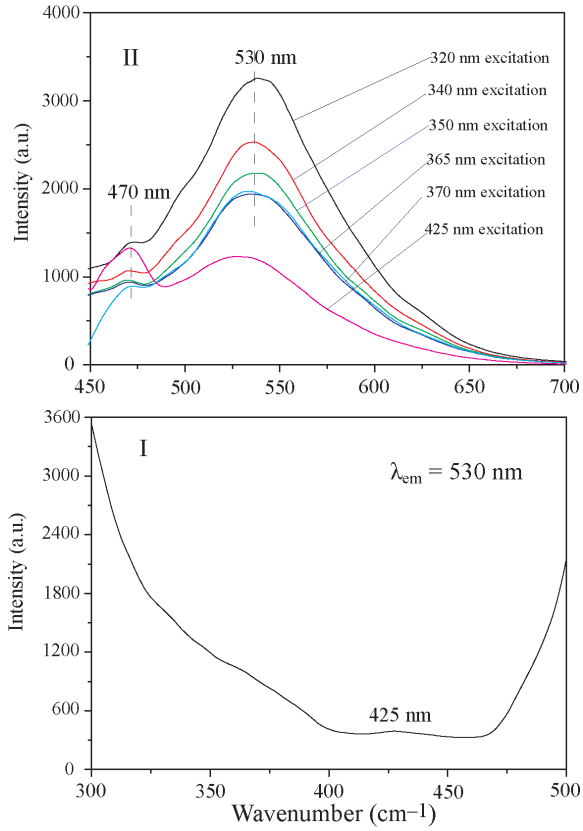

Figure 7. Excitation spectrum of CdS (λ_{em} = 530 nm) and emission spectra of Mag-CdS under different excitation wavelengths.

~530 nm and a weak peak at 470 nm under the excitations at 320, 340, 350, 365, 370, and 425 nm. The peak centered at 530 nm, which was associated with defect levels of interstitial sulfur (Vigil *et al.*, 1997; Blanco *et al.*, 1998), shifted by ~26 nm compared with

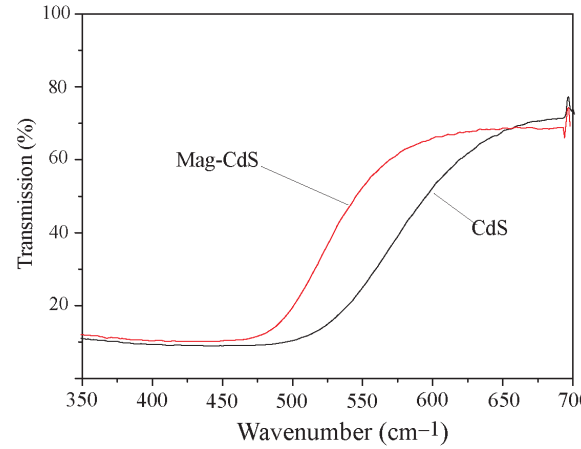

Figure 8. UV-visible spectra of Mag-CdS and CdS.

that of the pure CdS (556 nm), while the peak at 470 nm did not shift. (In PL or UV-vis spectra, a 'red shift' implies the position of a peak moving to lower energy or longer wavelength; 'blue shift' implies the position of a peak moving to higher energy or shorter wavelength.) Notably, no red PL bands occurred in the Mag-CdS composites. These red PL bands have been found in other composites consisting of CdS nanoparticles and inorganic host materials (Rosa-Fox *et al*., 2003; Guo *et a.l*, 2011; Kang *et al.*, 2008; Panda *et al.*, 2004), and thought to be related to the strain-related defects at the core/shell interface between CdS nanoparticles and inorganic host materials (Guo *et al.*, 2011). Various vacancies and interface defects between host materials and guests, however, often act as complicated luminescence centers and induce a wide variety of luminescence features for photon semiconductors (Cao *et al.*, 2005).

To understand the optical properties of the CdS nanoparticles before and after insertion into the Mag,

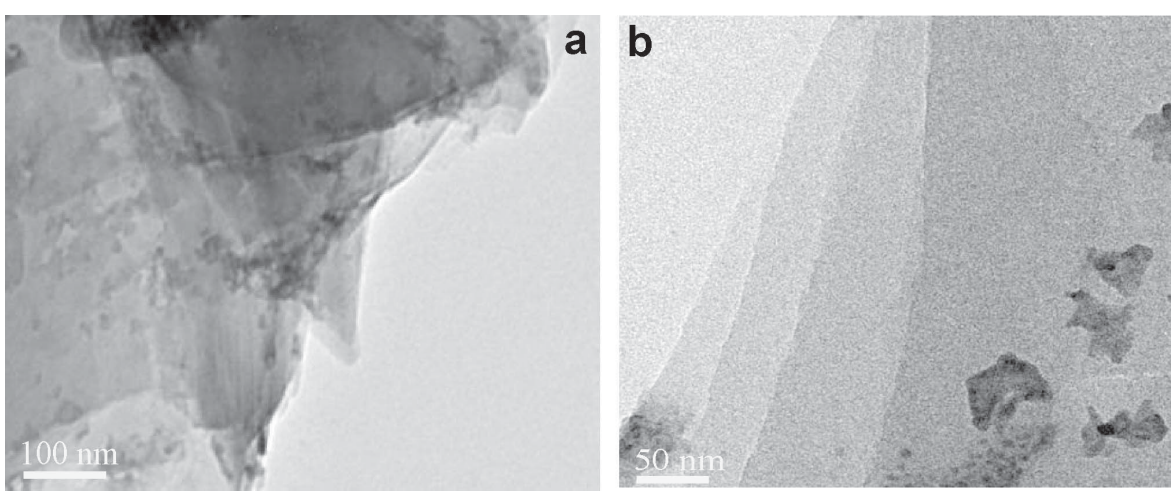

Figure 9. TEM observation of Mag-CdS at different magnifications.

UV-vis transmission spectra were recorded (Figure 8). The transmission band-edge of the Mag-CdS composite shifted to higher energy (2.4 eV, 525 nm) compared with that of the pure CdS particles (2.2 eV, 575 nm). The blue shift in the transmission spectra implied that the optical properties of CdS nanoparticles packed in the Mag may be modified by the host material.

To support these results, observation by TEM of the Mag-CdS composite (Figure 9) revealed a layered structure, with the sizes of particles in the Mag-CdS composites being <10 nm wide. Based on these results, the changed optical properties of CdS enclosed in Mag should be attributed largely to the effects of the host Mag on the CdS nanoparticles, such as size confinement effects or surface defects deactivation, *etc*.

CONCLUSIONS

The structure and optical properties of the composite based on CdS nanoparticles enclosed in layered magadiite were investigated. The blue shifts present in the PL and UV-vis transmission spectra for the Mag-CdS composite confirmed that the magadiite may modify the optical properties of CdS. Observation by TEM confirmed incorporation of CdS nanoparticles into magadiite and estimated the sizes of the enclosed CdS nanoparticles to be <10 nm across. The changed optical properties of the CdS nanoparticles enclosed in the magadiite may be due to the effects of the host magadiite on the CdS nanoparticles (such as size-confinement effect). The composite based on CdS nanoparticles enclosed in magadiite should be more resistant to acids than the pure CdS, and be more thermally stable than the composites based on CdS nanoparticles enclosed in organic hosts. The composite presented here has potential applications in optical fields.

ACKNOWLEDGMENTS

The present study was supported by the National Natural Science Foundation of China (Grant No.51162021).

REFERENCES

Aline, O.M. and Alexandre, G.S.P. (2009) Effect of thermal dehydration and rehydration on Na-magadiite structure. *Journal of Colloid and Interface Science*, **330**, 392−398.

Bases, C.F. and Mesmer Jr., R.E. (1976) *The Hydrolysis of Cations*. John Wiley & Sons, Inc., New York, pp. 300−301.

Bi, Y.F., Blanchard, J., Lambert, J.F., Millot, Y., Casale, S., Zeng, S., Nie, H., and Li, D.D. (2012) Role of the Al source in the synthesis of aluminum magadiite. *Applied Clay Science*, **57**, 71−78.

Blanco, A., López, C., Mayoral, R., Míguez, H., Meseguer, F., Mifsud, A., and Herrero, J. (1998) CdS photoluminescence inhibition by a photonic structure. *Applied Physics Letters*, **73**, 1781−1783.

Cao, L.X., Huang, S.H., Lü, S.Z., and Lin, J.L. (2005) Effect of layer thickness on the luminescence properties of ZnS/CdS/ZnS quantum dot quantum well. *Journal of Colloid Interface & Science*, **284**, 516−520.

Centi, G. and Perathoner, S. (2008) Catalysis by layered materials: A review. *Microporous and Mesoporous Materials*, **107**, 3−15.

Chang, S.Y., Liu, L., and Asher, S.A. (1994) Creation of templated complex topological morphologies in colloidal silica. *Journal of the American Chemistry Society*, **116**, 6745−6747.

Daily, J.S. and Pinnavaia, T.J. (1992) Intercalative reaction of a cobalt (III) cage complex, Co(sep) 3+, with magadiite, a layered sodium silicate. *Journal of Inclusion Phenomena and Molecular Recognition in Chemistry*, **13**, 47−61.

Díaz, U., Cantín, Á., and Corma, A. (2007) Novel layered organic-inorganic hybrid materials with bridged silsesquioxanes as pillars. *Chemistry of Materials*, **19**, 3686−3693.

Eugster, H.B. (1967) Hydrous sodium silicate from lake Magadi, Kenya: precursors for bedded chert. *Science*, **157**, 1177−1180.

Freeman, R., Gill, R., Beissenhirtz, M., and Willner, I. (2007) Self-assembly of semiconductor quantum-dots on electrodes for photoelectrochemical biosensing. *Photochemical and Photobiological Science*, **6**, 416−422.

Guerra, D.L., Ferrreira, J.N., Pereira, M.J., Viana, R.R., and Airoldi, C. (2010) Use of natural and modified magadiite as adsorbents to remove Th(IV), U(VI), and Eu(III) from aqueous media – thermodynamic and equilibrium study. *Clays and Clay Minerals*, **58**, 327−339.

Guo, L.M., Wang X.H., Zhong C.F., and Li, L.T. (2011) Synthesis and photoluminescence of CdS QDs in ZrO_2 nanotubes by sequential chemical bath deposition. *Journal of Physics D: Applied Physics*, **44**, 165403/1-5.

Huang, Y., Jiang, Z., and Schwieger,W. (1999) Vibrational spectroscopic studies of layered silicates. *Chemistry of Materials*, **11**, 1210−1217.

Jyothy, P.V., Amrutha, K.A., Xavier, J., and Unnikrishnan, N.V. (2009) Fluorescence characteristics of Dy^{3+}/CdS nanocrystals doped silica xerogel. *Journal of Physics and Chemistry of Solids*, **70**, 927−930.

Kang, S.Z., Cui, Z.Y., Xu, Z.Z., and Mu, J. (2008) Thermostability of photoluminescence of CdS nanoparticles loaded on silica spheres. *Colloids and Surfaces A: Physicochemical and Engineering Aspects*, **315**, 44−46.

Kryukov, A.I., Smirnova, N.P., Korzhak, A.V., Kuchmii, S.Ya., and Eremenko, A.M. (1998) CdS nanoparticles in porous silicate glasses: energy characteristics, photocatalytic activity, and the effect of siliver ion doping. *Theoretical and Experimental Chemistry*, **34**, 360−365.

Kwon, O.Y., Jeong, S.Y., Suh, J.K., and Lee, J.M. (1995) Hydrothermal synthesis of Na-magadiite and Na-kenyaite in the presence of carbonate. *Bulletin Korean Chemical Society*, **16**, 737−742.

Laughlin, R.B. and Joannopoulos, J.D. (1977) Phonons in amorphous silica. *Physical Review B*, **16**, 2942−2952.

Li, Y., Chun, E., Liu, Y., Pickett, N., Skabara, P.J., Cummins, S.S., Ryley, S., Sutherland, A.J., and O'Brien, P. (2005) Synthesis and characterization of CdS quantum dots in polystyrene microbeads. *Journal of Material Chemistry*, **15**, 1238−1243.

Macedo, T.S.R., Petrucelli, G.C., and Airoldi, C. (2007) Silicic acid magadiite as a host for n-alkyldiamine guest molecules and features related to the thermodynamics of intercalation. *Clays and Clay Minerals*, **55**, 151−159.

McAtee, J.L., House, R., and Eugster, H.P. (1968) Magadiite from Trinity County, California. *American Mineralogist*, **53**, 2061−2069.

Mizukami, N., Tsujimura, M., Kuroda, K., and Ogawa, M. (2002) Preparation and characteriza- tion of Eu-magadiite intercalation compounds. *Clays and Clay Minerals*, **50**, 799−806.

Motke, S.G., Yawale, S.P., and Yawale, S.S. (2002) Infrared

spectra of zinc doped lead borate glasses. *Bulletin of Material Science*, **25**, 75−78.

Nunes, A., Moura, A.O., and Prado, A.G.S. (2011) Calorimetric aspects of adsorption of pesticides 2,4-D, diuron and atrazine on a magadiite surface. *Journal of Thermal Analysis and Calorimetry*, **106**, 445−452.

Ogawa, M., Ide, Y., and Mizushima, M. (2010) Controlled spatial separation of Eu ions in layered silicates with different layer thickness. *Chemical Communications*, **46**, 2241−2243.

Ogawa, M. and Kuroda, K. (1995) Photofunctions of intercalation compounds. *Chemical Reviews*, **95**, 399−438.

Ozawa, K., Nakao, Y., Cheng, Z.X., Wang, D.F., Osada, M.R., Okada, R., Saeki, K., Itoh, H., and Iso, F. (2009) Fabrication of novel composites of ZnO-nanoparticles and magadiite. *Materials Letters*, **63**, 366−369.

Panda, S.K., Chakrabarti, S., Satpati, B., Satyam, P.V., and Chaudhuri, S. (2004) Optical and microstructural characterization of CdS−ZnO nanocomposite thin films prepared by sol−gel technique. *Journal of Physics D: Applied Physics*, **37**,628−635.

Park, K.W., Jung, J.H., Seo, H.J., and Kwon, O.Y. (2009) Mesoporous silica-pillared kenyaite and magadiite as catalytic support for partial oxidation of methane. *Microporous and Mesporous Materials*, **121**, 219−225.

Rai, S. and Bokatial, L. (2011) Effect of CdS nanoparticles on photoluminescence spectra of Tb^{3+} in sol−gel-derived silica glasses. *Bulletin of Material Science*, **34**, 227−231.

Rayevska, O.E., Grodzyuk, G.Y., Dzhagan, V.M., Stroyuk, O.L., Kuchmiy, S.Y., Plyusnin, V.F., Grivin, V.P., and Valakh, M.Y. (2010) Synthesis and characterization of white-emitting CdS quantum dots stabilized with polyethylenimine. *Journal of Physical Chemistry C*, **114**, 22478−22486.

Rosa-Fox, N.D., Piñero, M., Litrán, R., and Esquivias, L. (2003) Photoluminescence from CdS quantum dots in silica gel. *Journal of Sol-Gel Science and Technology*, **26**, 947−951.

Schwieger, W. and Lagaly, G. (2004) Alkali silicates and crystalline silicic acids. Pp. 541−551 in: *Handbook of Layered Materials* (S.M. Auerbach, K.A. Carrado, and P.K. Dutta, editors). Marcel Dekker Inc, New York.

Schwieger, W., Selvam, T., Gravenhorst, O., Pfänder, N., Schlögl, R., and Mabande, G.T.P. (2004) Intercalation of $[Pt(NH_3)_4]2t$ ions into layered sodium silicate magadiite: a useful method to enhance their stabilisation in a highly dispersed state. *Journal of Physics and Chemistry of Solids*, **65**, 413−420.

Shen, S. and Guo, L. (2008) Growth of quantum-confined CdS nanoparticles inside Ti-MCM-41 as a visible light photocatalyst. *Materials Research Bulletin*, **43**, 437−446.

Sun, W.T., Yu, Y., Pan, H.Y., Gao, X.F., Chen, Q., and Peng, L.M. (2008) CdS quantum dots sensitized TiO_2 nanotube-array photoelectrodes. *Journal of the American Chemical Society*, **130**, 1124−1125.

Sun, X., King, J., and Anthony, J.L. (2009) Molecular sieve synthesis in the presence of tetra-alkylammonium and dialkylimidazolium molten salts. *Chemical Engineering Journal*, **147**, 2−5.

Supronowicz, W., Roessner, F., Schwieger, W., Meilikhov, M., and Esken, D. (2012) Synthesis and properties of Sn-containing magadiite. *Clays and Clay Minerals*, **60**, 254−264.

Vigil, O., Reich, I., García-Rocha, M., and Zelaya-Ańgel, O. (1997) Characterization of defect levels in chemically deposited CdS films in the cubic-to-hexagonal phase transition. *Journal of Vacuum Science & Technology A*, **15**, 2282−2286.

Vorokh, A.S., Kozhevnikov, N.S., Uritskaya, A.A., and Magerl, A. (2008) The synthesis of nucleus−shell $Cd(OH)_2$/CdS structures by chemical precipitation from aqueous solutions. *Russian Journal of Physical Chemistry A*, **82**, 1132−1139.

Wang, Y., Meng, G., Zhang, L., Liang, C., and Zhang, J. (2002) Catalytic growth of large-scale single-crystal CdS nanowires by physical evaporation and their photoluminescence. *Chemistry of Materials*, **14**, 1773−1777.

Wei, F., Li, G.C., and Zhang, Z.K. (2005) Synthesis of high quality CdS nanorods by solvo-thermal process and their photoluminescence. *Journal of Nanoparticle Research*, **7**, 685− 689.

Xu, F., Yuan, Y.F., Han, H.J., Wu, D.P., Gao, Z.Y., and Jiang, K. (2012) Synthesis of ZnO/CdS hierarchical heterostructure with enhanced photocatalytic efficiency under nature sunlight. *CrystEngComm*, **14**, 3615−3622.

Zhao, P.Q., Xiong, S.J., Wu, X.L., and Chu, P.K. (2012) Photoluminescence induced by twinning interface in CdS nanocrystals. *Applied Physics Letters*, **100**, 171911/1-4.

Zhen, W. and Pinnavaia, T.J. (2003) Intercalation of poly(-propyleneoxide) amines (Jeffamines) in synthetic layered silicas derived from ilerite, magadiite, and kenyaite. *Journal of Material Chemistry*, **13**, 2127−2131.

(*Received 17 September 2012; revised 26 December 2012; Ms. 715; AE: S.M. Kuznicki*)